

HEAT TRANSFER ANALYSIS IN THE TIME-DEPENDENT AXISYMMETRIC STAGNATION POINT FLOW OVER A LUBRICATED SURFACE

Khalid MAHMOOD¹, Muhammad SAJID, Nasir ALI and Tariq JAVED

Department of Mathematics and Statistics, International Islamic University,
Islamabad 44000, Pakistan

Abstract: *In this paper time-dependent, two-dimensional, axisymmetric flow and heat transfer of a viscous incompressible fluid impinging orthogonally on a disc is examined. The disc is lubricated with a thin layer of power-law fluid of variable thickness. It is assumed that surface temperature of the disc is time-dependent. Continuity of velocity and shear stress at the interface layer between the fluid and the lubricant has been imposed to obtain the solution of the governing partial differential equations. The set of partial differential equations is reduced into ordinary differential equations by suitable transformations and are solved numerically by using Keller-Box method. Solutions are presented in the form of graphs and tables in order to examine the influence of pertinent parameters on the flow and heat transfer characteristics. An increase in lubrication results in the reduction of surface shear stress and consequently viscous boundary layer becomes thin. However, the thermal boundary layer thickness increases by increasing lubrication. It is further observed that surface shear stress and heat transfer rate at the wall enhance due to unsteadiness. The results for the steady case are deduced from the present solutions and are found in good agreement with the existing results in the literature.*

Keywords: *Axisymmetric stagnation point flow, power law fluid, Keller-Box method, heat transfer, lubricated surface.*

1 Introduction

In recent years many researchers working in the field of fluid dynamics are showing their interest in the study of fluids having nonlinear relationship between the shear stress and the rate of deformation. The reason of the increasing interest lies in the fact that most of the fluids that exist in nature and industry cannot be classified by Navier-Stokes equations. Particularly one cannot classify lubricants with the constitutive relationship of a Newtonian fluid. Axisymmetric orthogonal stagnation point flow is one of the classical problems in fluid mechanics. These jet-like flows of fluids impinging on a solid surface have number of industrial applications in order to transfer heat and/or mass. Examples include cooling

¹Corresponding author: Khalid Mahmood
e-mail address: khalidmeh2012@gmail.com

of gas turbine blades and photovoltaic cells, annealing of metals and cooling in grinding processes. The shear stress induced by the flowing fluid stream is used to clean the surface of plates, to manufacture paper and photographic films and to control the thickness in the wire coating process. The pioneering work on the axisymmetric stagnation-point flow was studied by Homann [1] and Frossling [2]. The three-dimensional orthogonal stagnation-point flow was carried out by Howarth [3] and Davey [4] as a special case. Yeckel et al. [5] discussed stagnation-point flow on a rigid plate against a thin lubrication layer for the first time. Blyth and Pozrikidis [6] studied stagnation-point flow of a viscous fluid past a liquid film on a plane wall.

The unsteady stagnation point flow over a flat plate was initially discussed by Yang [7]. After this, Williams [8] and Cheng et al. [9] investigated the axisymmetric three dimensional stagnation flow on a stationary disc. The unsteady MHD flow with heat transfer of a fluid film spread over a rotating infinite disc was encompassed by Kumari and Nath [10]. They obtained two solutions by taking thin and thick films of fluid. Nazar et al. [11] studied the time-dependent two-dimensional stagnation point flow over a flat stretching sheet moving with velocity proportional to the distance from stagnation point. The unsteady stagnation point flow with a span-wise oscillating wall was addressed by Fang and Lee [12]. Cheng and Dai [13] investigated the unsteady two-dimensional stagnation-point flow of a viscous fluid over a stretching sheet using homotopy analysis method. Unsteady stagnation-point flow over an impinging plate was discussed by Zhong and Fang [14] for the planar and axisymmetric flows. The unsteady flow past a stretching sheet is investigated by Pop and Na [15]. They proved that the unsteady flow approaches towards the steady flow situation for large times.

A solution of the Navier-Stokes and energy equations illustrating skin friction and temperature of an infinite plate was studied by Stuart [16]. Gorla [17] investigated heat transfer in an axisymmetric stagnation flow on a cylinder. Axisymmetric stagnation-point flow with heat transfer of a viscous fluid on a moving cylinder with unsteady axial velocity and uniform transpiration was analyzed by Saleh and Rahimi [18]. In another paper Abbasi and Rahimi [19] studied three-dimensional stagnation-point flow and heat transfer on a flat plate with transpiration. Recently Abbasi and Rahimi [20] carried out investigation of two-dimensional stagnation-point flow and heat transfer impinging on a flat plate. Massoudi and Razeman [21] studied heat transfer analysis of a viscoelastic fluid at a stagnation point. Elbashbeshy and Bazid [22] analyzed heat transfer due to an unsteady boundary layer flow over a stretching sheet and found that thermal and momentum boundary layer thickness depends upon unsteadiness parameter. Ishak et al. [23] discussed mixed convection stagnation point flow on a vertical stretching sheet and found that heat transfer rate at the surface increases with an increase in unsteadiness parameter.

In all above investigations the conventional no-slip has been imposed at fluid-solid interface. However, there are many situations where the no-slip boundary condition is not realistic and can be replaced by the linear slip boundary condition proposed by Navier [24] and Maxwell [25] independently. Typical examples are emulsions, foams, suspensions and polymer solutions. In 1980, Joseph [26] discussed

boundary conditions for thin lubrication layers. In another paper, Beavers and Joseph [27] discussed the slip boundary condition in detail. The stagnation-point flow subject to slip boundary condition that occurs in rarefied flow or under high pressure was carried out by Wang [28]. Two dimensional stagnation point flow of an elasto-viscous fluid with partial slip was investigated by P. D. Ariel [29]. Munawar et al. [30] discussed the slip effects in the flow between two stretchable discs by using an analytical method. The slip flow over a lubricated surface is considered by Solbakken and Anderson [31]. The slip boundary conditions for the viscous flow past a power-law lubricant was derived by Andersson and Rousselet [32] for the first time. They obtained the similarity solution numerically, for power-law lubricant by taking the value of power-law index $n = 1/3$. The axisymmetric stagnation point flow of a viscous fluid past a power-law lubricant has been discussed by Santra et al. [33]. Recently Sajid et al. [34] extended the work of Santra et al. for a generalized slip boundary condition. In another paper Sajid et al. [35] investigated stagnation-point flow of Walter' B fluid over a lubricated surface. The axisymmetric stagnation-point flow of a third grade fluids over a lubricated surface has been examined by Sajid et al. [36]. Mahmood et el. [37, 38] investigated flows of second grade fluids, respectively, near an oblique stagnation point due to a lubricated plate and over a lubricated rotating disc.

Our aim in the present investigation is to discuss time-dependent axisymmetric stagnation-point flow and heat transfer of a viscous fluid over a disc lubricated with power-law fluid. A new slip condition at the interface of the viscous and power- law fluid has been derived and results for no-slip and full-slip cases have been deduced from the obtained numerical solutions. The objective of the present study is to investigate the influence of slip parameter and unsteadiness parameter on the flow characteristics and heat transfer. The numerical solution is developed by using Keller-Box method [39-41].

2 Mathematical formulation

Let us assume the unsteady, two-dimensional, axisymmetric stagnation-point flow and heat transfer of an incompressible viscous fluid past a disc lubricated by a thin layer of non-Newtonian power law fluid. The origin O is located at the center of the disc.

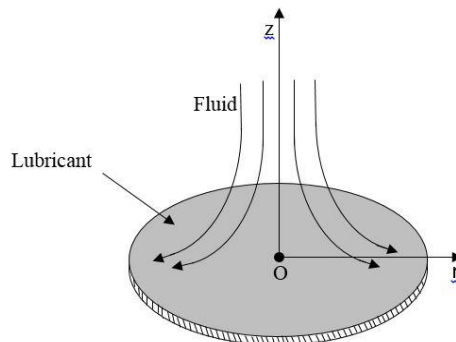


Fig. 1: Diagram showing stagnation point flow problem.

The flow rate Q of the lubricant coming out of a small point source at the center of the disc is given by

$$Q = \int_0^{\delta(r)} U(r, z) \cdot 2\pi r dz, \quad (1)$$

where $U(r, z)$ is the radial component of the velocity vector $\mathbf{V} = [U, V, W]$ of power-law fluid and $\delta(r)$ is the variable thickness of the lubrication layer. The circumferential velocity component $V(r, z)$ has no contribution in the radial direction. The stagnation flow velocity of the viscous fluid is of the form $u_\infty(r, z, t) = ar/(1 - \beta t)$ where $a > 0$ and $\beta > 0$ are constants with dimensions t^{-1} . T_w is the time-dependent temperature of the disc and is given as

$$T_w = T_\infty + T_0(1 - \beta t)^{-3/2}, \quad (2)$$

where T_∞ is constant free stream temperature and the constant T_0 is the measure of rate of increase in the temperature along the disc. Under these assumptions, the unsteady, two-dimensional, axisymmetric flow of bulk fluid is governed by the following equations

$$\frac{\partial u}{\partial r} + \frac{u}{r} + \frac{\partial w}{\partial z} = 0, \quad (3)$$

$$\frac{\partial u}{\partial t} + u \frac{\partial u}{\partial r} + w \frac{\partial u}{\partial z} = -\frac{1}{\rho} \frac{\partial P}{\partial r} + \nu \left(\frac{\partial^2 u}{\partial r^2} + \frac{\partial}{\partial r} \left(\frac{u}{r} \right) + \frac{\partial^2 u}{\partial z^2} \right), \quad (4)$$

$$\frac{\partial w}{\partial t} + u \frac{\partial w}{\partial r} + w \frac{\partial w}{\partial z} = -\frac{1}{\rho} \frac{\partial P}{\partial z} + \nu \left(\frac{\partial^2 w}{\partial r^2} + \frac{1}{r} \frac{\partial w}{\partial r} + \frac{\partial^2 w}{\partial z^2} \right), \quad (5)$$

$$\frac{\partial T}{\partial t} + u \frac{\partial T}{\partial r} + w \frac{\partial T}{\partial z} = \alpha \left(\frac{\partial^2 T}{\partial r^2} + \frac{1}{r} \frac{\partial T}{\partial r} + \frac{\partial^2 T}{\partial z^2} \right), \quad (6)$$

where u and w are the velocity components in the cylindrical polar coordinate system (r, θ, z) , $P(r, z)$ is the fluid pressure, ρ is the fluid density, ν is kinematic viscosity and α is thermal diffusivity. At free stream, $u = u_\infty(r, z, t)$ and therefore Eq. (4) reduces to

$$\frac{\partial u}{\partial t} + u \frac{\partial u}{\partial r} + w \frac{\partial u}{\partial z} = \frac{\partial u_\infty}{\partial t} + u_\infty \frac{\partial u_\infty}{\partial r} + \nu \left(\frac{\partial^2 u}{\partial r^2} + \frac{\partial}{\partial r} \left(\frac{u}{r} \right) + \frac{\partial^2 u}{\partial z^2} \right), \quad (7)$$

The appropriate boundary conditions at $z = 0$ for the present flow situation is discussed in detail by Santra et al. [33] and are

$$\frac{\partial u}{\partial z} = \frac{k}{\mu} \left(\frac{\pi}{Q} \right)^n r^n (ru)^{2n}, \quad P(r, \delta(r), t) = -\frac{\rho r^2}{2} \left(\frac{a}{1 - \beta t} \right)^2, \quad w(r, \delta(r), t) = 0 \quad (8)$$

The boundary conditions far away from the stagnation point in the present case are given by

$$u(r, z, t) = u_\infty = \frac{ar}{1 - \beta t}, \quad w(r, z, t) = -\frac{2az}{1 - \beta t}. \quad (9)$$

The boundary conditions to be satisfied by the temperature are

$$T(r, z) = T_w \text{ at } z = 0 \text{ and } T(r, z) \rightarrow T_\infty \text{ as } z \rightarrow \infty. \quad (10)$$

Introducing the dimensionless variables

$$\eta = \sqrt{\frac{a}{v(1-\beta t)}} z, \quad u = U_\infty f'(\eta), \quad w = -2 \sqrt{\frac{av}{(1-\beta t)}} f(\eta), \quad (11)$$

$$P = \frac{\mu}{r} u_\infty p(\eta) - \frac{\rho r^2}{2} \left(\frac{a}{1-\beta t} \right)^2, \quad T - T_\infty = (T_w - T_\infty) \theta(\eta) \quad (12)$$

the flow is governed by

$$f'''' + 2ff'' - (f')^2 + A \left(1 - f' - \frac{\eta}{2} f'' \right) + 1 = 0, \quad (13)$$

$$p' + 4ff' + 2f'' - A(\eta f' + f) = 0, \quad (14)$$

$$\theta'' + Pr \left\{ 2f\theta' - \frac{A}{2} (3\theta + \eta\theta') \right\} = 0, \quad (15)$$

$$f(0) = 0, \quad p(0) = 0, \quad f''(0) = \lambda (f'(0))^{\frac{2}{3}}, \quad f'(\infty) = 1, \quad (16)$$

$$\theta(0) = 1, \quad \theta(\infty) = 0. \quad (17)$$

where prime denotes the differentiation with respect to η . $A = \beta/a$ is the unsteadiness parameter and $Pr = \nu/\alpha$ is the Prandtl number. For $A = 0$, the problem reduces to the steady state case discussed by Santra et al. [33]. The parameter λ given in Eq. (16) is given by

$$\lambda = \frac{k\sqrt{v}}{\mu} \left(\frac{\pi}{Q} \right)^{\frac{1}{3}} \frac{b^{\frac{2}{3}}}{b^{\frac{3}{2}}} = \frac{\sqrt{\frac{v}{b}}}{\frac{\mu(Qb)^{\frac{1}{3}}}{k}} = \frac{L_{visc}}{L_{lub}}, \quad (18)$$

in which $b = a/(1 - \beta t)$. It is worth mentioning that we have taken $n = 1/3$ as discussed by Santra et al. [33]. It is clear from Eq. (18) that λ is the ratio between the viscous length scale L_{visc} and lubrication length scale L_{lub} . For the case when the lubrication length L_{lub} is small, the parameter λ becomes large. In the limiting case when $\lambda \rightarrow \infty$, the conventional no-slip condition $f'(0) = 0$, is obtained from Eqs. (16). On the other hand when L_{lub} is large, λ becomes small. In the limiting case when $\lambda \rightarrow 0$, one obtains the full slip boundary condition $f''(0) = 0$ from Eqs.(16). Hence λ is an inverse measure of slip and is known as slip parameter.

3 Numerical results and discussions

To see the influence of pertinent parameters on the velocity components, pressure and temperature, Eqns. (13)-(15) subject to boundary conditions (16)-(17) are solved numerically by using Keller-Box method [39-41]. The numerical results are validated through the comparison of the present solution with the existing results in the literature in the special cases.

Figures. 2-11 are plotted to observe the effects of emerging parameters on velocity components, pressure distribution and temperature profile. Numerical computations for surface shear stress and heat transfer rate showing the influence of parameters λ , A and Pr are presented in tables 1-2.

To see the effects of slip parameter λ on f , f' and $-p$, figs. 2-4 have been plotted. The dashed lines in each case are the investigations of Santra et al. [33] when $A = 0$. Figure 2 is displayed to show the effects of λ on axial velocity component f . From this figure, it is clear that as we increase the slip on the surface (λ is decreased), an increase in the value of f is observed. f becomes proportional to η as $\lambda \rightarrow 0$ i.e. when full-slip is applied on the surface. Figure 3 is displayed to see the influence of slip parameter λ on the radial velocity component f' . We see that f' decreases by increasing λ . It is due to the fact that lubrication reduces the friction on the surface. It is also clear from figs. 2-3 that power-law lubricant enhances the velocity of fluid at the surface. The variation of the pressure profiles $-p$ with η is presented in fig. 4. For the case of no-slip (classical Homann flow), the pressure increases towards the surface in the stagnation zone and it obtains a minimum value at $\eta = 0$. The pressure variation across the boundary layer is increased with increasing slip, and the maximum pressure build-up is observed for full-slip. The pressure increase is slightly slow in the boundary layer region for the no-slip case. As we increase the slip on the surface, the boundary layer thickness reduces and pressure seems to increase rapidly. It is clear from fig. 4 that the pressure curves intersect slightly beyond $\eta = 1$ when $A = 0$. If we inspect the graph closely, we notice that the crossings of the different curves do not occur in one single point. It is evident from eq. (14) that the pressure is function of both the radial and the axial velocity components, which in turn depends upon the slip. The point of inflection produced by pressure distribution is observed somewhat above the surface for the no-slip case. As we increase the slip on the surface, this inflection point seems to shift towards the surface. But when $A = 1$, the point of inflection moves beyond $\eta = 1.57$ (solid lines) showing that boundary layer thickness increases by increasing the numerical value of parameter A .

Effect of parameter A both for no-slip and partial-slip cases on the velocity components and pressure profile is illustrated in figs. 5-7. Figure 5 shows that magnitude of axial velocity f increases by increasing A for both cases. It is also evident from this figure that lubrication appreciates the effects of A (solid lines). Figure 6 elucidates the effects of parameter A on the radial velocity component f' both for no-slip (dashed lines) and partial-slip (solid lines) cases. It is observed from this figure that as A increases, f' increases. Moreover the lubricated surface enhances the effect of A (solid lines). i.e. Increase in the radial velocity becomes more rapid by lubricating the surface. The effects of unsteadiness

parameter A on pressure profile is depicted in fig. 7. The dashed lines are for no-slip case and solid lines for partial-slip case. This figure shows that the pressure increases by decreasing A and is maximum when $A = 0$. It has also been observed that the increase in the pressure becomes more significant by applying slip on the surface.

Variation of θ for different values of A when $Pr = 1$ both for no-slip (dashed lines) and partial slip (solid lines) cases is elaborated in fig. 8. It is evident from this figure that θ decreases by increasing A . This decrease can be enhanced by applying the lubrication on the surface ($\lambda = 1$). Figure 9 depicts the variation in the magnitude of θ for different values of slip parameter λ when $Pr = 1$ both for steady ($A = 0$) and unsteady ($A = 2$) cases. It is concluded from this figure that θ increases with an increase in the value of λ (by decreasing amount of lubrication). This figure also shows that unsteadiness depreciates the effects of lubrication (solid lines). The influence of Pr on temperature profile is elucidated in fig. 10 when $A = 1$ both for no-slip and partial slip cases. According to this figure as Pr is increased, a decrease in the numerical value of θ is observed which further depreciates on the lubricated surface (solid lines). Figure 11 is devoted for the effects of Pr on temperature θ by considering steady and unsteady cases respectively. It has been noted from this figure that θ decreases by increasing Pr . It is also clear from this figure that as unsteadiness increases, more decrease in the magnitude of temperature is seen.

Numerical values of the skin friction coefficient at the surface for various values of λ and A are illustrated in the table 1 and are compared with [33] when $A = 0$. It is evident from this table that $f''(0)$ decrease by increasing slip on the surface and increase by increasing unsteadiness parameter A . Hence the slip on the surface causes a decrease in the value of skin friction coefficient as expected. The variation in local Nusselt number under the influence of different parameters is presented in table 2. It is clear from the table 2 that $-\theta'(0)$ decreases by increasing slip parameter and increases by increasing unsteadiness parameter and Prandtl number.

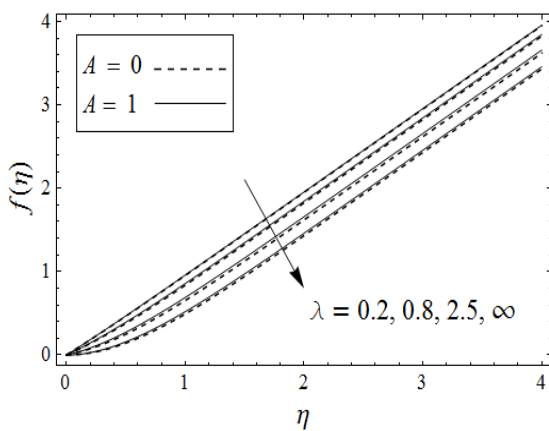


Fig. 2. Variation of $f(\eta)$ for different values of λ when $A = 0$ and $A = 1$.

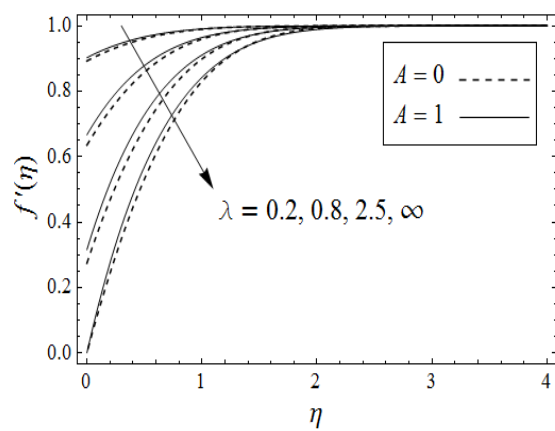


Fig. 3. Variation of $f'(\eta)$ for different values of λ when $A = 0$ and $A = 1$.

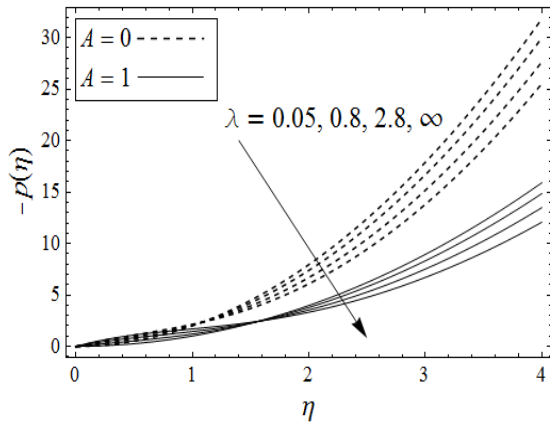


Fig. 4. Variation of $-p(\eta)$ for different values of λ when $A = 0$ and $A = 1$.

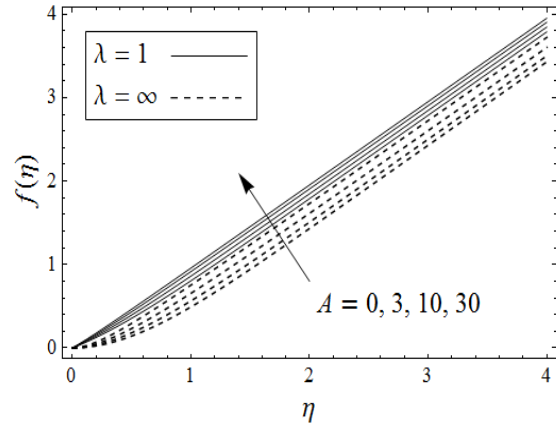


Fig. 5. Variation of $f(\eta)$ for different values of A when $\lambda = 1$ and $\lambda = \infty$.

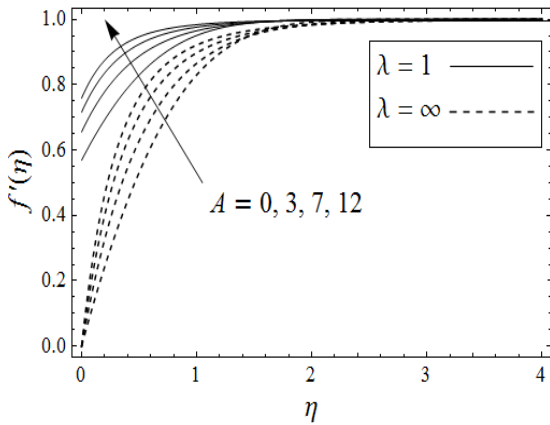


Fig. 6. Variation of $f'(\eta)$ for different values of A when $\lambda = 1$ and $\lambda = \infty$.

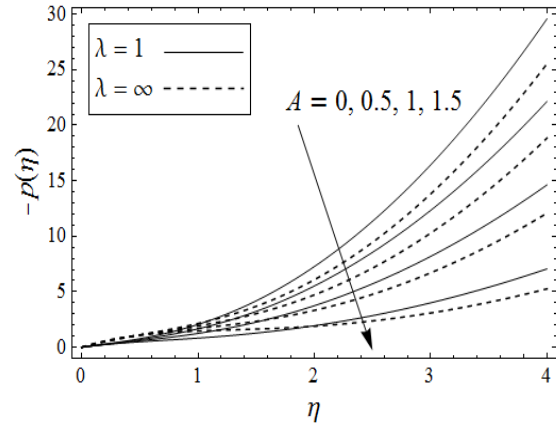


Fig. 7. Variation of $-p(\eta)$ for different values of A when $\lambda = 1$ and $\lambda = \infty$.

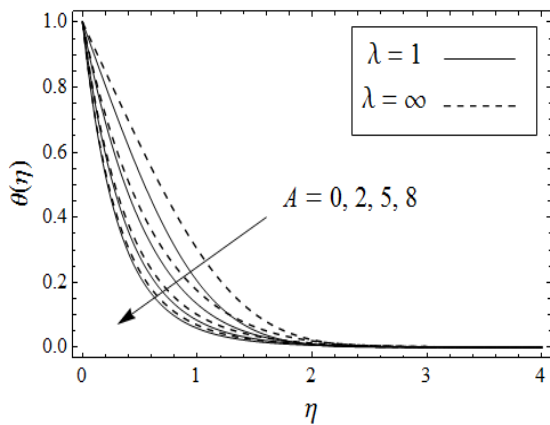


Fig. 8. Variation of $\theta(\eta)$ for different values of A and λ when $Pr = 1$.

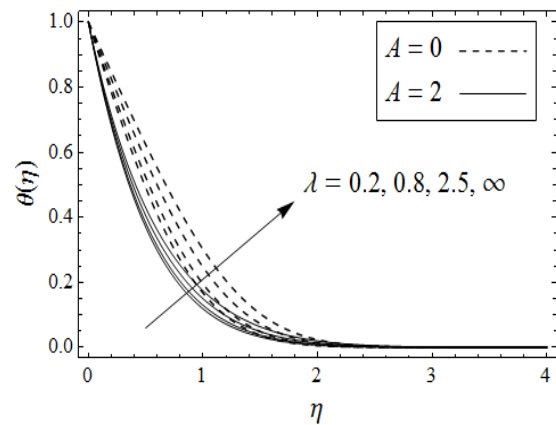


Fig. 9. Variation of $\theta(\eta)$ for different values of λ and A when $Pr = 1$.

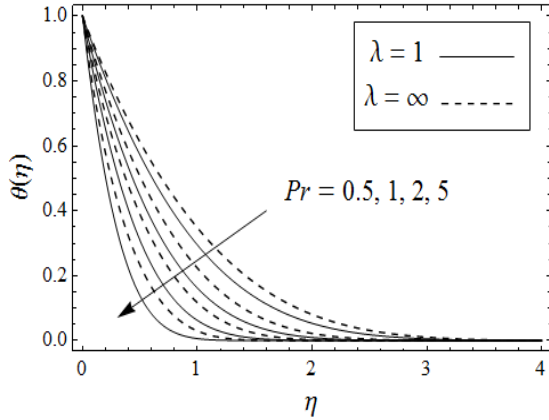


Fig. 10. Variation of $\theta(\eta)$ for different values of Pr and λ when $A = 1$.

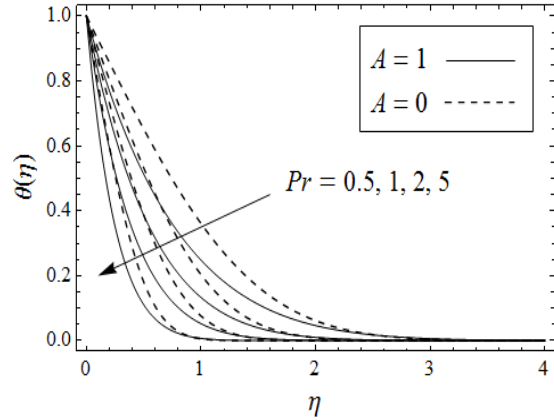


Fig. 11. Variation of $\theta(\eta)$ for different values of Pr and A when $\lambda = 1$.

Table 1: Numerical values for the skin friction coefficient $f''(0)$ for various values of λ and A . The values in the parenthesis are given by Santra et al. [33].

λ	$A = 0$	$A = 1$	$A = 5$	$A = 50$	$A = 100$
0.01	0.009994 (0.009993)	0.009995	0.009996	0.009998	0.009999
0.05	0.049245 (0.049246)	0.049254	0.049364	0.049744	0.049815
0.1	0.096639 (0.096638)	0.096645	0.097474	0.098978	0.099264
0.5	0.414733 (0.414732)	0.421773	0.440708	0.475200	0.481994
1	0.687618 (0.687618)	0.714975	0.780883	0.904371	0.929885
2	0.979046 (0.979048)	1.058510	1.249381	1.643876	1.733929
5	1.211821 (1.211820)	1.384896	1.854787	3.175248	3.567803
10	1.275873 (1.275870)	1.491554	2.129354	4.484463	5.404635
50	1.308716 (1.308716)	1.550981	2.313818	6.112016	8.336686
100	1.310810 (1.310810)	1.554897	2.327023	6.281861	8.712896
500	1.311853 (1.311853)	1.556854	2.333675	6.371818	8.920022
∞	1.311956 (1.311956)	1.557046	2.334332	6.380862	8.941168

Table 2: Numerical values for the $-\theta'(0)$ for various values of Pr .

Pr	$\lambda = 0.1$ $A = 1$	$\lambda = 1$ $A = 1$	$\lambda = \infty$ $A = 1$	$A = 0$ $\lambda = 1$	$A = 10$ $\lambda = 1$	$A = 100$ $\lambda = 1$
0.1	0.500049	0.487277	0.461699	0.366244	1.161069	3.578919
0.5	1.078508	1.028799	0.933355	0.714680	2.591787	8.001272
1	1.523383	1.440575	1.284502	0.985666	3.663082	11.31356
2	2.152020	2.018342	1.770419	1.359311	5.177554	15.99468
5	3.398468	3.157204	2.717160	2.083981	8.181352	25.26648
10	4.802738	4.435593	3.772494	2.888600	11.56521	35.67804
50	10.73049	9.816135	8.193578	6.244961	25.82568	78.82254

100	15.17721	13.84586	11.49833	8.749920	36.47870	109.8120
-----	----------	----------	----------	----------	----------	----------

4 Conclusion

In this paper, we have investigated heat transfer analysis in the time-dependent axisymmetric stagnation point flow over a disc lubricated with power-law fluid. We have taken $n = 1/3$ so that results can be compared in the special case. The numerical solutions of the governing nonlinear equations together with nonlinear boundary conditions are developed using Keller-Box method. The motivation is to determine the effect of the slip parameter λ and unsteadiness parameter A on the flow characteristics. Main findings of the present study are

- (i) Numerical values of f and f' increase by increasing the unsteadiness parameter A and by decreasing slip parameter λ .
- (ii) Temperature θ increases with an increase in λ and decreases for large values of A and Pr .
- (iii) The skin friction coefficient increases by increasing both λ and A . Thus slip on the surface causes a decrease in the value of skin friction coefficient.
- (iv) Heat transfer rate at the wall decreases with an increase in the value of slip parameter, however, it increases by increasing A and Pr .

References

- [1] Homann, F., Der Einfluss grosser Zahigkeit bei der Stromung um den Zylinder und um die Kugel, *Z. angew. Math. Mech. (ZAMM)*, 16 (1936), pp. 153–164
- [2] Frossling, N., Verdunstung, Wärmeübertragung und Geschwindigkeitsverteilung bei zweidimensionaler und rotationssymmetrischer laminarer Grenzschichtstromung, *Lunds Univ. Arsskr. N.F. Avd.*, 2 (1940), 35, No. 4
- [3] Howarth, L., The boundary layer in three-dimensional flow. Part II: The flow near a stagnation point, *Phil. Mag. VII*, 42 (1951), pp. 1433–1440
- [4] Davey, A., Boundary layer flow at a saddle point of attachment, *J. Fluid Mech.*, 10 (1961) pp. 593–610
- [5] Yeckel, A., Strong, L., Middleman, S., Viscous film flow in the stagnation region of the jet impinging on planar surface, *AIChE J.*, 40 (1994), pp.1611–1617
- [6] Blyth, M. G., Pozrikidis, C., Stagnation-point flow against a liquid film on a plane wall, *Acta Mech.*, 180 (2005), pp. 203–219
- [7] Yang, K. T., Unsteady laminar boundary layers in an incompressible stagnation flow, *ASME Journal of Applied Mechanics*, 25 (1958), pp. 421–427
- [8] Williams, J. C., Non-steady stagnation-point flow, *AIAA Journal*, 6 (12), (1968), pp.2417–2419
- [9] Cheng, E. H. W., Ozisik, M. N., and Williams, J. C., Non-steady three-dimensional stagnation point flow, *ASME Journal of Applied Mechanics*, 38 (1971), pp. 282–287

- [10] Kumari, M., Nath, G., Unsteady MHD film flow over a rotating infinite disk, *International Journal of Engineering Science*, 42 (2004), pp. 1099–1117
- [11] Nazar, R., Amin, N., Filip, D., Pop, I., Unsteady boundary layer flow in the region of the stagnation point on a stretching sheet, *International Journal of Engineering Science*, 42 (2004), pp. 1241–1253
- [12] Fang, T., Lee, C. F., Three-dimensional wall-bounded laminar boundary layer with span-wise cross free stream and moving boundary, *Acta Mechanica*, 204 (2009), pp. 235–248
- [13] Cheng, J., Dai, S. Q., A uniformly valid series solution to the unsteady stagnation-point flow towards an impulsively stretching surface, *Science in China Series G: Physics, Mechanics & Astronomy*, 53 (2010), pp. 521–526
- [14] Zhong, Y., Fang, T., Unsteady stagnation-point flow over a plate moving along the direction of flow impingement, *International Journal of Heat and Mass Transfer*, 54 (2011), pp. 3103–3108
- [15] Pop, I., Na, T. Y., Unsteady flow past a stretching sheet, *Mech. Res. Comm.*, 23 (1996), pp. 413–422
- [16] Stuart, J. T., A solution of the Navier-Stokes and energy equations illustrating the response of skin friction and temperature of an infinite plate thermometer to fluctuations in the stream velocity, *Proceedings of The Royal Society of London. Series A*, 231 (1955), pp. 116–130
- [17] Gorla, R. S. R., Heat transfer in an axisymmetric stagnation flow on a cylinder, *Applied Scientific Research*, 32 (1976), pp. 541–553
- [18] Saleh, R., Rahimi, A. B., Axisymmetric stagnation-point flow and heat transfer of a viscous fluid on a moving cylinder with time-dependent axial velocity and uniform transpiration, *Journal of Fluids Engineering*, 126 (2004), pp. 997–1005
- [19] Shokrgozar Abbasi, A., Rahimi, A. B., Three-dimensional stagnation-point flow and heat transfer on a flat plate with transpiration, *Journal of Thermophysics and Heat Transfer*, 23 (2009), pp. 513–521
- [20] Shokrgozar Abbasi, A., Rahimi, A. B., Investigation of two-dimensional stagnation-point flow and heat transfer impinging on a flat plate, *Journal of Heat Transfer*, 134 (2012), pp. 024501-1–024501-6
- [21] Massoudi, M., Razeman, M., Heat transfer analysis of a viscoelastic fluid at a stagnation point, *Mech. Res. Commun.*, 19 (1992), pp. 129–134
- [22] Elbashbeshy, E. M. A., Bazid, M. A. A., Heat Transfer over an Unsteady Stretching Surface, *Journal of Heat and Mass Transfer*, 41 (2004), pp. 1-4
- [23] Ishak, A., Nazar, R., Pop, I., Mixed convection on the stagnation point flow towards a vertical continuously stretching sheet, *ASME J Heat Transfer*, 129 (2007), pp. 1087–1090
- [24] Navier, HMLC. Memoire sur les lois du mouvement des fluides. Memoires de l'Academie Royale des Sciences de l'Institut de France, 6 (1823), pp. 389–440

- [25] Maxwell, J. C., On stresses in rarified gases arising from inequalities of temperature, *Phil. Trans. Roy. Soc. London*, 170 (1879), pp. 231–256
- [26] Joseph, D. D., Boundary conditions for thin lubrication layers, *Phys. Fluids*, 23 (1980) pp. 2356–2358
- [27] Beavers, G.S., Joseph, D.D., Boundary Conditions at a Naturally Permeable Wall, *Journal of Fluid Mechanics*, 30 (1967), pp. 197– 207
- [28] Wang, C. Y., Stagnation flows with slip: exact solutions of the Navier–Stokes equations. *Z. Angew. Math. Phys. (ZAMP)*, 54 (2003), pp. 184–189
- [29] Ariel, P. D., Two dimensional stagnation point flow of an elastico-viscous fluid with partial slip, *Z. Angew. Math. Mech. (ZAMM)*, 88 (2008), pp. 320–324
- [30] Munawar, S., Mehmood, A., and Ali, A., Effects of slip on flow between two stretchable disks using optimal homotopy analysis method, *Canadian Journal of Applied Sciences*, 1 (2011), pp. 50–68
- [31] Solbakken, S., Anderson, H. I., Slip flow over lubricated surfaces, *Flow Turbol. Combust.*, 73 (2004), pp. 77–93
- [32] Andersson, H. I., Rousselet, M., Slip flow over a lubricated rotating disc, *Int. J. Heat Fluid Flow*, 27 (2006), pp. 329–335
- [33] Santra, B., Dandapat, B. S., Andersson, H. I., Axisymmetric stagnation-point flow over a lubricated surface, *Acta Mech.*, 194 (2007), pp. 1–10
- [34] Sajid, M., Mahmood, K., Abbas, Z., Axisymmetric stagnation point flow with a general slip boundary condition over a lubricated surface, *Chinese Physics Letters*, 29 (2012), 024702
- [35] Sajid, M., Javed, T., Abbas, Z., Ali, N., Stagnation-point Flow of a Viscoelastic Fluid over a Lubricated Surface, *Int. J. Nonlinear Sci. Numer. Simul.*, 14 (2013), pp. 285–290
- [36] Sajid, M., Ahmed, M., Ahmad, I., Taj, M., Abbasi, A., Axisymmetric stagnation-point flow of a third grade fluid over a lubricated surface, *Advances in Mechanical Engineering*, 7 (2015), pp.1–8
- [37] Mahmood, K., Sajid, M., Ali, N., Non-orthogonal Stagnation-point Flow of a Second-grade Fluid Past a Lubricated Surface, *ZNA*, 71 (2016), pp. 273-280
- [38] Mahmood, K., Sajid, M., Ali, N., Javed, T., Slip flow of a second grade fluid past a lubricated rotating disc, *International Journal of Physical Sciences*, 11 (2016), pp. 96-103
- [39] Keller, H. B., Cebeci, T., Accurate Numerical Methods for Boundary Layer Flows II: Two Dimensional Turbulent Flows, *American Institute of Aeronautics and Astronautics*, 10 (1972), pp.1193–1199
- [40] Bradshaw, V., Cebeci, T. and Whitelaw, I. H., Engineering Calculation Methods for Turbulent Flows, *Academic, London*, (1981)
- [41] Keller, H. B. A., New Difference Scheme for Parabolic Problems, in Numerical Solution of Partial Differential Equations (J. Bramble, ed.), *Volume II, Academic, New York*, (1970)